Energy migration processes in phosphate nanocrystals: size and dimensionality dependence

N.V. Kononets, V.V. Seminko, P.O. Maksimchuk, I.I. Bespalova, V.K. Klochkov, and Yu.V. Malyukin

Institute for Scintillation Materials, National Academy of Sciences of Ukraine,
60 Nauky Ave., Kharkiv 61072, Ukraine
E-mail: seminko@isma.kharkov.ua

Peculiarities of electronic excitation energy migration in phosphate nanocrystals with three-dimensional ($EuPO_4$) and one-dimensional (EuP_3O_9) arrangement of regular ions under variation of concentration of both energy traps (Nd^{3+} ions) and scattering centres (La^{3+} ions) are discussed in the paper. Processes of energy migration in both $EuPO_4$ and EuP_3O_9 nanocrystals are phonon-assisted ones due to absence of resonance between energy levels of adjacent Eu^{3+} ions. The distance of energy migration for both $EuPO_4$ and EuP_3O_9 nanocrystals was found to be equal to tens of nanometres, however, for $EuPO_4$ nanocrystals energy migration leads to stronger quenching of Eu^{3+} luminescence. For 10 nm $EuPO_4$ nanocrystals sufficient hampering of energy migration is observed due to the depletion of the low-energy phonon spectrum as a result of the phonon confinement effect.

1. Introduction

Development of biological labels for visualization of intra-cellular processes has recently made sufficient advances providing biologists with high number of various materials ranging from fluorescent dyes to inorganic nanoparticles. A number of newly developed biomedical techniques such as visualization of deep tumors and x-ray photodynamic therapy require scintillating RE-doped inorganic nanoparticles [1,2]. Using the mechanisms of transport of electronic excitation energy within the system of rare-earth (RE) ions, energy absorbed by nanoparticle can be delivered either to photosensitizer molecules chemically or physically absorbed on the surface of nanoparticle, or to other rare-earth ions which IR luminescence can deeply penetrate into biological tissue. So, the peculiarities of migration of electronic excitation energy over sublattice of regular RE ions should be taken into account for development of more efficient nanomaterials for these needs.

Phosphate nanoparticles have recommended themselves as the excellent materials for biomedical applications [3–5]. For instance, calcium phosphate nanoparticles have shown good biocompatibility and absence of toxicity being easily dissolved in lysosomes after the cellular intake [6,7].

Both arrangement of regular RE ions [8,9] and size of nanocrystal can provide the sufficient modification of the process of electronic excitation energy migration. For the sufficient small sizes the nanocrystal surface can play a role of scattering impurities providing the localization of electronic excitation inside the "cage" and in this way leading to increase of the probability of electronic excitation energy capture by traps [10,11]. Also, in our last studies for Pr^{3+}-doped silicate [12], vanadate [13], and phosphate [14] nanocrystals, we have observed that dopant ions with radii different from the ones of regular ions are preferably localized in the near-surface layer of nanoparticle. So, for effective delivery of energy absorbed within nanoparticle to luminescence centers the distance of energy migration must be comparable with the size of nanocrystal itself. From all RE-doped crystals, only the ones containing Eu^{3+}, Tb^{3+} and Gd^{3+} as regular ions have shown the energy migration over sufficient distances (1 nm or more) [15–17], while for other RE ions luminescence is quenched effectively by cross-relaxation mechanism [18,19] and any sufficient migration of energy cannot be expected.

In this paper we have investigated the migration of electronic excitation energy in Nd^{3+} and La^{3+}-doped phosphate nanoparticles ($EuPO_4$ and EuP_3O_9) with different arrangements of regular Eu^{3+} ions (three-dimensional for $EuPO_4$ and one-dimensional for EuP_3O_9) and sizes. Migration of electronic excitation energy in some

phosphate crystals and micropowders were investigated previously in the number of papers [20,21]. However, recent studies have shown that the mechanisms of excitation energy relaxation in RE-doped nanoparticles can differ sufficiently from the ones for bulk crystals leading, for instance, to modification of kinetics of luminescence decay [22], absorption/emission from high stark components [23,24] and abnormal narrowing of spectral lines [25]. For undoped $EuPO_4$ and EuP_3O_9 nanocrystals the processes of energy migration were studied in our previous paper [26]. In this paper, using the variation of the concentrations of Nd^{3+} and La^{3+} ions in $EuPO_4$ and EuP_3O_9 nanocrystals we have determined the role of both the arrangement of regular Eu^{3+} ions and nanocrystal size in the formation of specific features of the migration of electronic excitation energy in these nanocrystals.

2. Experimental

In order to obtain 100 nm $EuPO_4$ and $Eu_{1-x}La_xPO_4:Nd^{3+}$ (0.1, 0.7, 1.5 at.%) nanocrystals H_3PO_4 solution (0.5 mol/l) was added to 10 ml $EuCl_3$ solution (0.5 mol/l) till $EuPO_4$ precipitation. After centrifugation the precipitate was annealed at 1100 °C in air during 5 h.

For the synthesis of 10 nm $EuPO_4$ nanocrystals colloidal aqueous solutions of rare-earth chloride and sodium tripolyphosphate were used. Sodium tripolyphosphate played the dual role — as the source of PO_4^{3-} anions formed during tripolyphosphate hydrolysis and as stabilizing agent for colloidal nanoparticle. Details of synthesis are described in our previous paper [27].

EuP_3O_9 and $Eu_{1-x}La_xP_3O_9:Nd^{3+}$ nanocrystals with different concentration of neodymium ions (0.1, 0.7, 1.5 at.%) were synthesized by solid state method. Europium (III) oxide (Eu_2O_3), lanthanum (III) oxide (La_2O_3), neodymium (III) oxide (Nd_2O_3) and ammonium dihydrophosphate ($NH_4H_2PO_4$) taken in required proportions were milled in agate mortar, then heated to 600 °C with heating speed of 50 °C/h and maintained at this temperature for 10 h. Then the powder again was grounded in an agate mortar, and annealed at 1000 °C for 15 h. Average size of synthesized nanocrystals was ~ 100 nm.

The purity of crystal phase was controlled by x-ray diffraction (XRD) (Fig. 1). The sizes of nanocrystals were determined using transmission electron microscopy (TEM) and ZetaPALS analyzer (Brookhaven, NY). In the Fig. 2 TEM images of $EuPO_4$ nanocrystals of different sizes are shown.

Luminescence spectra were obtained using spectrofluorimeter based on the grating monochromator, luminescence was excited by the fourth harmonics of YAG:Nd laser ($\lambda_{exc} = 266$ nm).

The luminescence decay was taken using the time-correlated single-photon counting (TCSPC) technique. Temperature was varied from 10 to 300 K using ARS
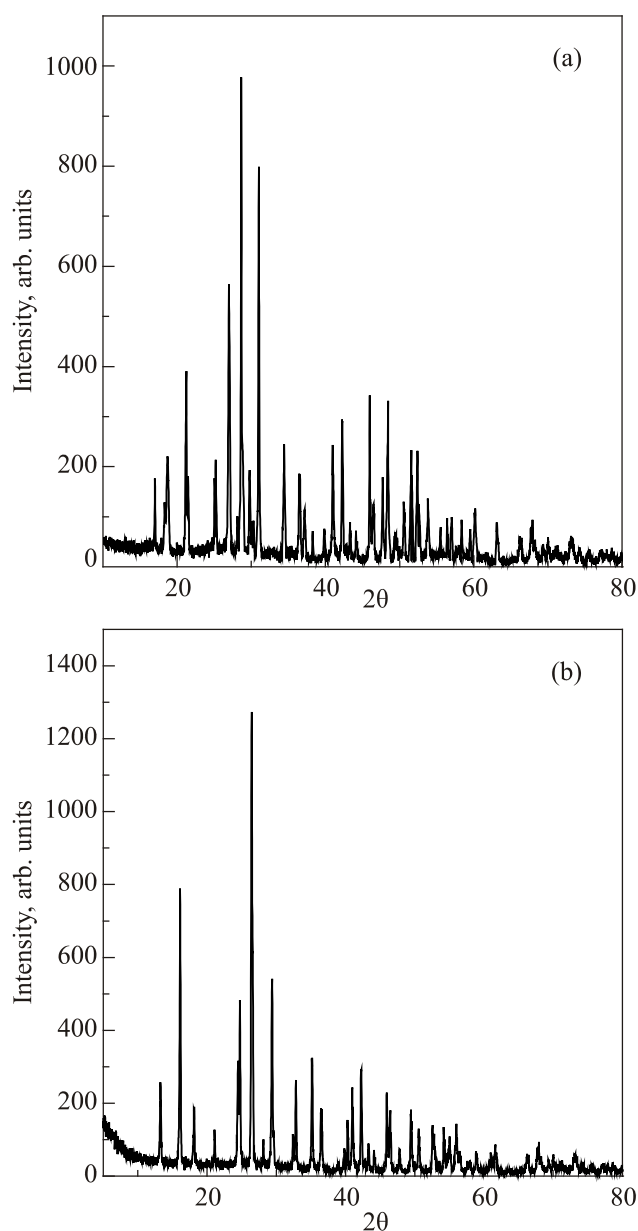

Fig. 1. XRD of $EuPO_4$ (a) and EuP_3O_9 (b) nanocrystals.

DE-204AE cryostat with LakeShore 335 temperature controller.

3. Results and discussion

The crystal structure of EuP_3O_9 is characterized by presence of one-dimensional Eu^{3+} chains with ~4.2 Å distance between Eu^{3+} ions in the same chain and ~7.3 Å between chains [28] and previously, in [29] it was shown that energy migration in bulk EuP_3O_9 is strongly anisotropic. At the same time, the structure of $EuPO_4$ does not involve any anisotropy in arrangement of regular ions (shortest distance between Eu^{3+} ions ~3.5 Å) [30]. In order to compare the peculiarities of electronic excitation energy migration in phosphate nanocrystals with different structures we have used Nd^{3+}-doped mixed $La_{1-x}Eu_xPO_4$ and $La_{1-x}Eu_xP_3O_9$

which concentration is unknown, doping by Nd^{3+} ions (0.1, 0.7 and 1.5 at.%) was used for creation of intentionally determined concentrations of energy traps. Variation of La^{3+} content was used to estimate the distance of energy migration in both types of nanocrystals.

The luminescence spectra of Nd^{3+}-doped (0.1 at.%) $EuPO_4$ and EuP_3O_9 nanocrystals (λ_{exc} = 266 nm) are shown in the Fig. 4. The spectra consist of spectral lines corresponding to the characteristic $^5D_0 \rightarrow {}^7F_J$ (J = 0, 1, 2, 3) transitions of Eu^{3+} ions (Fig. 4). Spectral lines of Nd^{3+} ions cannot be observed in the spectra (Nd^{3+} luminescence is in the IR region). For $EuPO_4$:Nd^{3+} nanocrystals both temperature and

Fig. 2. TEM images of 100 (a) and 10 (b) nm $EuPO_4$ nanocrystals.

nanocrystals, where Nd^{3+} ions were used as energy traps, and La^{3+} ions as scattering centers (energy barriers) (see Fig. 3). For the investigation of the influence of size restriction on the processes of energy migration 100 nm and 10 nm $EuPO_4$ nanocrystals were obtained. Because, in pure EuP_3O_9 and $EuPO_4$ nanocrystals energy traps are represented by europium (Eu^{3+}) ions with distorted coordination,

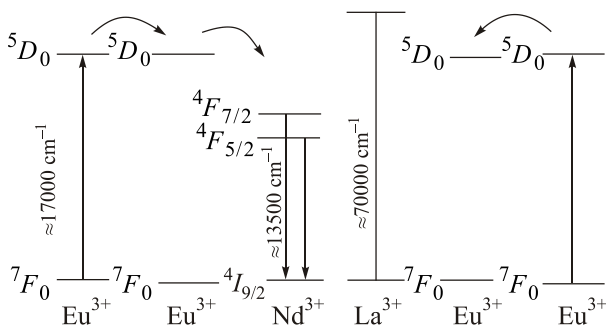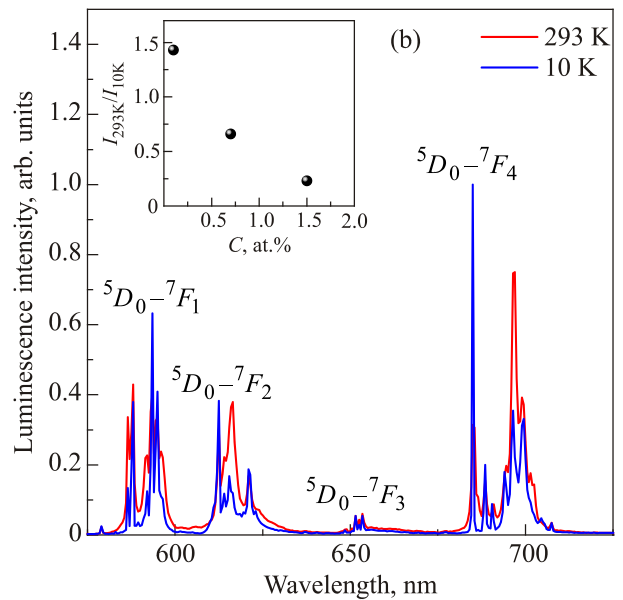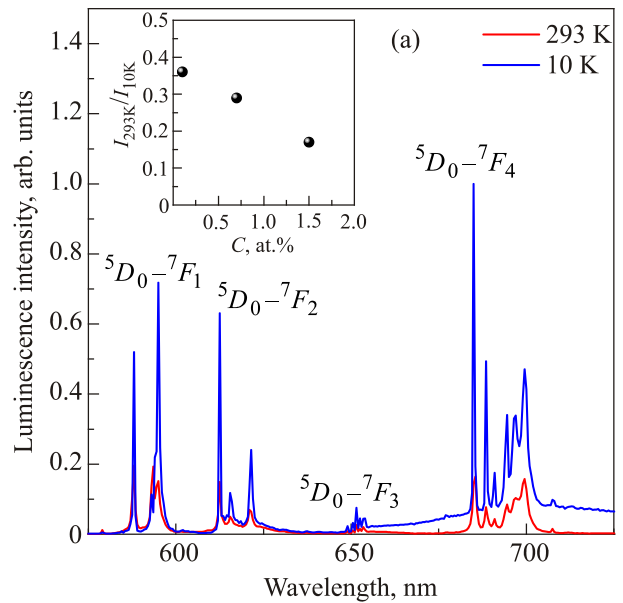*Fig. 3.* Scheme of energy levels and possible pathways of energy migration in Nd^{3+}-doped mixed $La_{1-x}Eu_xPO_4$ and $La_{1-x}Eu_xP_3O_9$ nanocrystals.

Fig. 4. (Color online) Luminescence spectra of Nd^{3+}-doped (0.1 at.%) $EuPO_4$ (a) and EuP_3O_9 (b) nanocrystals at 10 and 293 K (λ_{exc} = 266 nm). Insets: Nd^{3+} concentration dependence of I_{293K}/I_{10K} ratio for $EuPO_4$ and EuP_3O_9 nanocrystals, respectively.

N.V. Kononets, V.V. Semink, P.O. Maksimchuk, I.I. Bespalova, V.K. Klochkov, and Yu.V. Malyukin

Nd^{3+} concentration increase leads to Eu^{3+} luminescence quenching due to energy transfer from Eu^{3+} to Nd^{3+} ions (Fig. 4(a)). In the insets the changes of I_{293K}/I_{10K} ratio for $EuPO_4$ and EuP_3O_9 nanocrystals with variation of Nd^{3+} concentration are shown, where I_{10K} and I_{293K} are the integrated Eu^{3+} $^5D_0\rightarrow{}^7F_J$ luminescence intensities at 10 and 293 K, respectively. For Nd^{3+}-doped $EuPO_4$ nanocrystals the stronger Eu^{3+} luminescence quenching is observed as compared to Nd^{3+}-doped EuP_3O_9 nanocrystals with the same dopant concentration (for 0.7 at.%: I_{293K}/I_{10K} ~ 0.3 for $EuPO_4$:Nd^{3+} and ~ 0.7 for EuP_3O_9:Nd^{3+}, for 1.5 at.%: I_{293K}/I_{10K} ~ 0.15 for $EuPO_4$:Nd^{3+} and ~ 0.25 for EuP_3O_9:Nd^{3+}). The stronger luminescence quenching for nanocrystals with three-dimensional arrangement of Eu^{3+} ions can be explained by more effective excitation energy migration in such systems.

More information regarding energy migration parameters in $EuPO_4$ and EuP_3O_9 nanocrystals can be obtained from decay curves of $^5D_0$ luminescence of Eu^{3+} ions. Decay curves after 266 nm excitation were taken in the wide temperature range for Nd^{3+}-doped (0.1, 0.7 and 1.5 at.%) $EuPO_4$ and EuP_3O_9 nanocrystals. The decay for Nd^{3+} concentration equal to 0.1 at.% are shown in the Fig. 5(a) ($EuPO_4$) and Fig. 5(b) (EuP_3O_9). Both temperature and Nd^{3+} concentration increase led to stronger deviation of decay curves from single-exponential decay law. Time dependences of luminescence intensity in the presence of diffusion-limited energy migration are described by the following expressions: $I = I_0\exp(-t/\tau_0 - Wt)$, where W is proportional to traps concentration C (for three-dimensional energy migration) and $I = I_0\exp(-t/\tau_0 - Bt^{1/3})$, where B is proportional to $C^{2/3}$ (for one-dimensional energy migration) [31]. Analysis of decay curves for $EuPO_4$ and EuP_3O_9 nanocrystals at different temperatures and Nd^{3+} concentrations have shown that they are well-fitted by the corresponding decay laws (see insets in Figs. 5(a) and Fig. 5(b)). Energy migration parameters W and B depend both on Nd^{3+} concentration and temperature, but these dependences for $EuPO_4$ and EuP_3O_9 nanocrystals are sufficiently different (see Figs. 6(a) and 6(b)). While for EuP_3O_9 nanocrystals at all Nd^{3+} concentrations W increases only from 10 to 100 K after which no increase (or even slight decrease) of W is observed, for $EuPO_4$ W increases in the whole temperature range.

Also the change of the values of energy migration parameters with temperature variation is sufficiently different: up to 100 times for $EuPO_4$ and only 1.5 times for EuP_3O_9. These differences in temperature dependence confirm that energy migration lead to more effective quenching for $EuPO_4$ nanocrystals than for EuP_3O_9 ones in full agreement with the results obtained from luminescence spectra (Fig. 4). This, in turn, can be determined by different mechanisms of energy migration in $EuPO_4$ and EuP_3O_9 nanocrystals. For EuP_3O_9 the short separation between Eu^{3+} ions in the same chain favors energy migration via
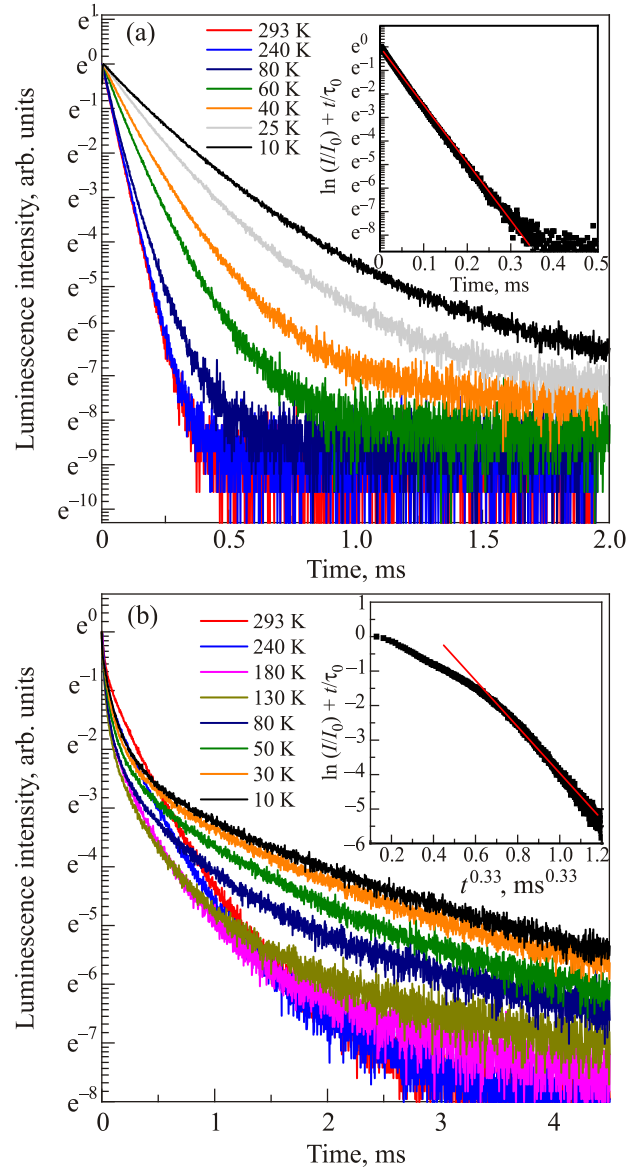

Fig. 5. (Color online) Decay curves of Nd^{3+}-doped (0.1 at.%) $EuPO_4$ (a) and EuP_3O_9 (b) nanocrystals at temperatures from 10 to 293 K (λ_{exc} = 266 nm). Insets: the same decay curves in $\{\ln(I/I_0)+t/\tau_0,\ t\}$ (for $EuPO_4$:Nd^{3+}) and $\{\ln(I/I_0)+t/\tau_0,\ t^{0.33}\}$ (for EuP_3O_9:Nd^{3+}) coordinates.

exchange interaction involving $^5D_0\rightarrow{}^7F_0$ transitions (in multipole approximation $^5D_0\rightarrow{}^7F_0$ transitions are absolutely forbidden as $0\rightarrow0$ transitions) [15]. Dipole-dipole interactions via $^5D_0\rightarrow{}^7F_1$ transitions cannot be completely ruled out, but even at room temperature, they should not lead to one-dimensional energy migration over any considerable distances. Really, for realization of this mechanism of energy migration, $^7F_1$ energy levels of high number of adjacent Eu^{3+} ions must be thermally populated. At 293 K the quota of ions with thermally populated $^7F_1$ energy levels is ~$\exp(-\Delta E/kT)$. The energy difference between $^7F_1$ and $^7F_0$ levels $\Delta E \approx 200$ cm^{-1}, so at room temperature $\exp(-\Delta E/kT) \approx \exp(-200/200) \approx 0.37$. Sure, this quota of
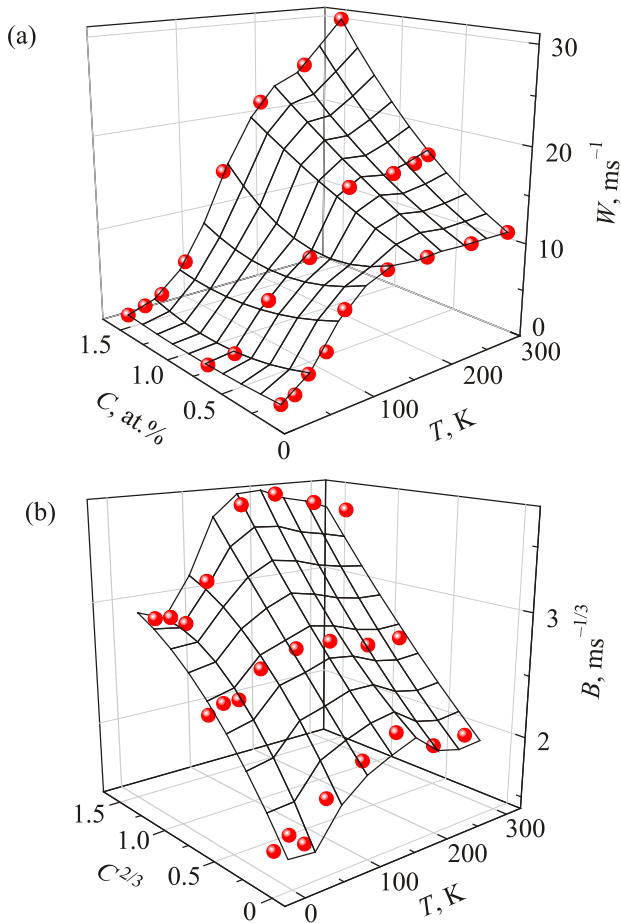
Fig. 6. (Color online) Temperature and Nd^{3+} concentration dependences of energy migration parameters W and B (described in the text) for $EuPO_4$ (a) and EuP_3O_9 (b) nanocrystals, respectively.

ions is insufficient for observing continual one-dimensional migration via dipole-dipole mechanism. So, the role of temperature in energy transfer processes consists only in overcoming the slight energy difference between $^5D_0$ levels of adjacent Eu^{3+} ions.

For $EuPO_4$ energy transfer via both multipole (dipole-dipole) and exchange interactions is possible. At low temperatures, energy migration is mainly determined by exchange interaction involving $^5D_0 \rightarrow {}^7F_0$ transitions, for which the role of temperature is limited to overcoming of small energy mismatch between adjacent Eu^{3+} ions. At higher temperatures, the thermal population of $^7F_1$ electronic levels becomes crucial. The quota of ions with thermally populated $^7F_1$ energy levels at room temperature as well as for EuP_3O_9 nanocrystals should be ≈ 0.37. However, contrary to EuP_3O_9 nanocrystals, energy migration in $EuPO_4$ nanocrystals is not limited to only one specific direction, so the dipole-dipole mechanism of energy migration via $^5D_0 \rightarrow {}^7F_1$ transitions is possible. In this way, the strong temperature dependence of energy migration in the whole temperature range is observed for $EuPO_4$ nanocrystals.

Distance of energy migration can vary sufficiently depending on the crystal structure. If this distance is comparable with the size of nanocrystal, influence of size restriction on the processes of energy migration can be expected. Presence or absence of such influence can be determined directly by obtaining nanocrystals with different sizes or by incorporation of energy barriers into Eu^{3+} chains. Decay curves of $La_{1-x}Eu_xPO_4$ and $La_{1-x}Eu_xP_3O_9$ nanocrystals with La^{3+} concentration of 0.1, 1, 10 and 50 at.% and fixed Nd^{3+} concentration of 0.1 at.% are shown in the Fig. 7. La^{3+} ions were supposed to play the same roles in the processes of energy migration as the boundaries of nanocrystal restricting the energy migration.

For $La_{1-x}Eu_xP_3O_9:Nd^{3+}$ decay curve at 50 at.% of La^{3+} ions was single exponential and no energy transfer was observed. This result agrees well with the previous supposition
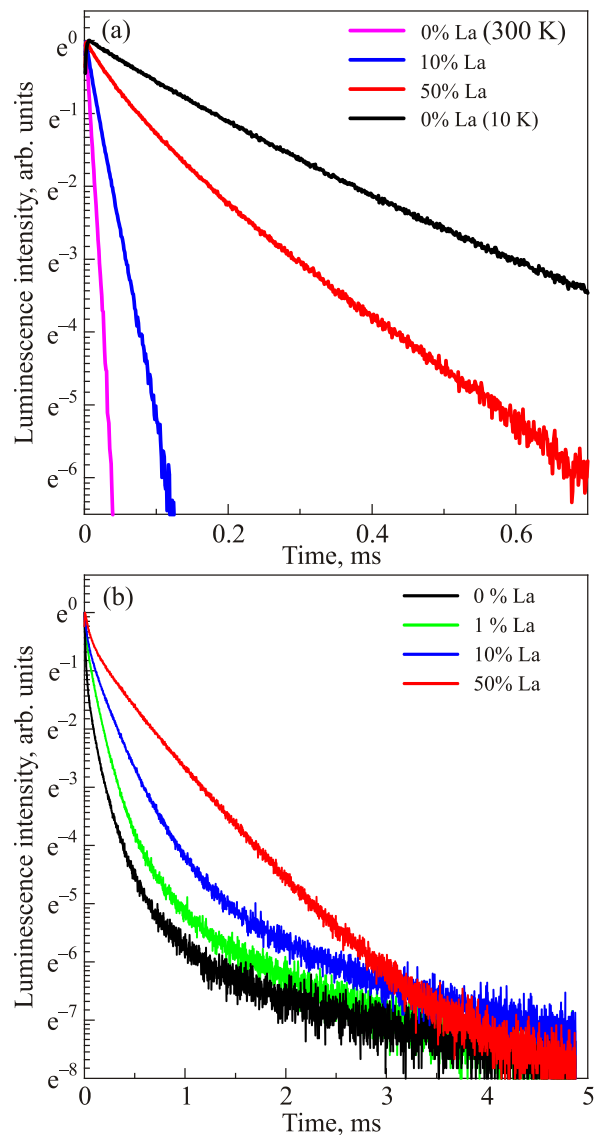

Fig. 7. (Color online) Decay curves of Nd^{3+}-doped (0.1 at.%) $La_{1-x}Eu_xPO_4$ (a) and $La_{1-x}Eu_xP_3O_9$ (b) nanocrystals with different La^{3+} concentration.

of exchange (and not dipole-dipole) interaction mediating energy transfer for EuP_3O_9. Contrary to $La_{1−x}Eu_xP_3O_9$:Nd^{3+}, for $La_{1−x}Eu_xPO_4$:Nd^{3+} decay curve at 50 at.% of La^{3+} ions was not single exponential due to possibility of dipole-dipole energy transfer mechanism. Decrease of La^{3+} content for both $La_{1−x}Eu_xP_3O_9$:Nd^{3+} and $La_{1−x}Eu_xPO_4$:Nd^{3+} leads to deviation of decay curves from exponential law. Decay curves for $EuPO_4$:Nd^{3+} and $La_{0.99}Eu_{0.01}PO_4$:Nd^{3+} coincide, while for $La_{1−x}Eu_xP_3O_9$:Nd^{3+} presence of even 1 at.% of La^{3+} ions leads to hampering of energy migration. Taking into account the distance between nearest-neighbor Eu^{3+} ions (3.5 Å for $EuPO_4$ and 4 Å for EuP_3O_9), one can conclude that the distance of energy migration within Eu^{3+} subsystem for both these structures is ~10 nm (for EuP_3O_9 — few tens nm) and variation of the size of nanocrystal would lead to modification of energy migration processes in these lattices.

As the distance of energy migration is comparable with the size of nanocrystal, decrease of the size of nanocrystal can lead to modification of energy migration process. In order to reveal directly the influence of size confinement on the energy transfer processes, $EuPO_4$ nanocrystals of different sizes were obtained. The decay curves for 10 and 100 nm $EuPO_4$ nanocrystals at temperature variation are shown in the Fig. 8 (inset). Decrease of the size of nanocrystal leads to shortening of the average distances between initially excited Eu^{3+} ions and quenching sites (first of all, surface-related defects such as near-surface Eu^{3+} ions with distorted coordination). So, according to our predictions, more effective quenching of Eu^{3+} luminescence should be observed. Surprisingly, decrease of the size of nanocrystal from 100 to 10 nm led to the hampering

of energy migration processes. Decay curve for 10 nm $EuPO_4$ nanocrystal was close to single exponential at 10 K and in contrast to 100 nm $EuPO_4$ nanocrystals increase of the temperature did not led to any sufficient decrease of decay time. So, energy migration to quenching sites via Eu^{3+} sublattice becomes less efficient for small $EuPO_4$ nanocrystals.

This effect, however, can be explained taking into account the influence of the nanocrystal size on the phonon spectra [22] and peculiarities of energy migration via Eu^{3+} ions revealed before [15,29]. Luminescence spectra of 10 nm $EuPO_4$ nanocrystals are characterized by sufficient inhomogeneous broadening of Eu^{3+} spectral lines as compared to the luminescence spectra of 100 nm nanocrystals (Fig. 8). Increase of the spectral width of Eu^{3+} lines for 10 nm nanocrystals can be determined by high number of Eu^{3+} ions with irregular coordination (first of all, near-surface Eu^{3+} ions and Eu^{3+}-oxygen vacancy complexes). As was mentioned before, the processes of energy migration in 100 nm $EuPO_4$ nanocrystals are phonon-assisted ones due to absence of resonance between energy levels of adjacent Eu^{3+} ions. Role of lattice phonons is even higher for 10 nm $EuPO_4$ nanocrystals, for which inhomogeneous broadening is sufficient (so, the energy mismatch between adjacent Eu^{3+} ions can be in the range of few tens $cm^{−1}$).

Phonon-assisted energy transfer processes in which energy migration requires lattice phonons can be sufficiently affected by the modification of phonon density of states (PDOS) in nanocrystals [22]. Analysis of the possible vibrational modes for the finite sphere [32,33] has shown the presence of so-called cutoff frequency in the phonon spectra (leading to absence of low-energy vibrational modes) and modification of PDOS spectra as a whole. Experimental evidences of the influence of phonon spectra modification on the energy relaxation processes were obtained recently for nanoparticles with sizes 20 nm and less [16,17]. The effect of size restriction on the energy migration in $EuPO_4$ nanocrystals observed in our research can be ascribed to modification of phonon spectra as well. As the energy positions of $^5D_0$ level for Eu^{3+} ions differ from site to site, participation of phonons in energy migration is crucial and absence of phonon modes required for phonon-assisted energy transfer between these ions can lead to hampering of energy migration processes. So, the observed decay curves for 10 nm $EuPO_4$ nanocrystals remained close to single exponential in the wide temperature range.

Fig. 8. (Color online) Luminescence spectra of 100 and 10 nm $EuPO_4$ nanocrystals ($T = 10$ K). Inset: decay curves of 100 and 10 nm $EuPO_4$ nanocrystals at 10 and 293 K.

4. Conclusions

Investigation of excitation energy migration in europium phosphate nanocrystals with different sizes and arrangement of regular ions has shown that the processes of energy migration are sufficiently dependent on both these characteristics. Stronger quenching of $^5D_0$ luminescence of
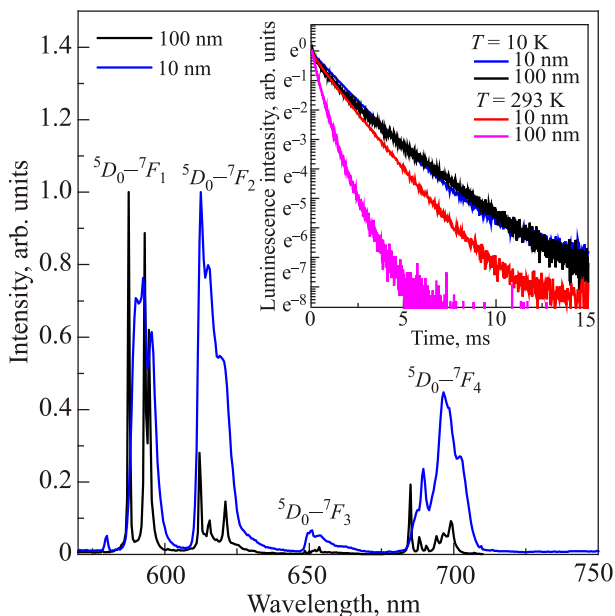
Eu^{3+} ions observed for $EuPO_4:Nd^{3+}$ nanocrystals as compared with $EuP_3O_9:Nd^{3+}$ nanocrystals is ascribed to different mechanisms of energy transfer between Eu^{3+} ions in these structures. Excitation energy migration for both $EuPO_4$ and EuP_3O_9 nanocrystals requires participation of low-energy phonons. In this way, decrease of the size of $EuPO_4$ nanocrystal to 10 nm leads to hampering of excitation energy migration due to the depletion of phonon spectra from the lower-frequency side for 10 nm nanoparticle.

––––––––

1. H. Chen, G.D. Wang, Y.J. Chuang, Z. Zhen, X. Chen, P. Biddinger, and J. Xie, *Nano Lett.* **15**, 2249 (2015).

2. S.L. Yefimova, T.N. Tkacheva, P.O. Maksimchuk, I.I. Bespalova, K.O. Hubenko, V.K. Klochkov, A.V. Sorokin, and Yu.V. Malyukin, *J. Lumin.* **192**, 975 (2017).

3. M. Epple, K. Ganesan, R. Heumann, J. Klesing, A. Kovtun, S. Neumann, and V. Sokolova, *J. Mater. Chem.* **20**, 18 (2010).

4. V. Uskoković and D.P. Uskoković, *J. Biomed. Mater. Res.* **96**, 152 (2011).

5. G. Bao, S. Mitragotri, and S. Tong, *Annu. Rev. Biomed. Eng.* **15**, 253 (2013).

6. I. Roy, S. Mitra, A. Maitra, and S. Mozumdar, *Int. J. Pharm.* **250**, 25 (2003).

7. E.I. Altınoglu, T.J. Russin, J.M. Kaiser, B.M. Barth, P.C. Eklund, M. Kester, and J.H. Adair, *ACS Nano* **2**, 2075 (2008).

8. P.A.M. Berdowski and G. Blasse, *J. Lumin.* **29**, 243 (1984).

9. M. Buijs and G. Blasse, *J. Lumin.* **34**, 263 (1986).

10. V.M. Kenkre, *Exciton Dynamics in Molecular Crystals and Aggregates*, Springer, Berlin, Heidelberg (1982).

11. A.A. Avedeenko, V.A. Karachevtsev, and Y.V. Naboikin, *J. Appl. Spectrosc.* **46**, 377 (1987).

12. V.V. Seminko, A.A. Masalov, Y.I. Boyko, and Y.V. Malyukin, *J. Lumin.* **132**, 2443 (2012).

13. V.V. Seminko, A.A. Masalov, Y.I. Boyko, and Y.V. Malyukin, *Opt. Mater.* **34**, 1998 (2012).

14. V.V. Seminko, P.O. Maksimchuk, N.V. Kononets, A.A. Masalov, Yu.I. Boyko, and Y.V. Malyukin, *Funct. Mater.* **19**, 309 (2012).

15. M. Buijs, A. Meyerink, and G. Blasse, *J. Lumin.* **37**, 9 (1987).

16. K.S. Sohn, Y.Y. Choi, H.D. Park, and Y.G. Choi, *J. Electrochem. Soc.* **147**(6), 2375 (2000).

17. A.J. De Vries, H.S. Kiliaan, and G. Blasse, *J. Solid State Chem.* **65**(2), 190 (1986).

18. Y.V. Malyukin, A.A. Masalov, P.N. Zhmurin, N.V. Znamenskii, E.A. Petrenko, and T.G. Yukina, *Phys. Status Solidi B* **240**(3), 655 (2003).

19. Y. Guyot, R. Moncorge, L.D. Merkle, A. Pinto, B. McIntosh, and H. Verdun, *Opt. Mater.* **5**(1–2), 127 (1996).

20. H. Meyssamy, K. Riwotzki, A. Kornowski, S. Naused, and M. Haase, *Adv. Mater.* **11**(10), 840 (1999).

21. K. Riwotzki, H. Meyssamy, H. Schnablegger, A. Kornowski, and M. Haase, *Angew. Chem. Int. Ed.* **40**(3), 573 (2001).

22. X.Y. Chen, H.Z. Zhuang, G.K. Liu, S. Li, and R.S. Niedbala, *J. Appl. Phys.* **94**(9), 5559 (2003).

23. G.K. Liu, H.Z. Zhuang, and X.Y. Chen, *Nano Lett.* **2**(5), 535 (2002).

24. Y.V. Malyukin, A.A. Masalov, and P.N. Zhmurin, *Opt. Commun.* **239**(4), 409 (2004).

25. P.O. Maksimchuk, A.A. Masalov, V.V. Seminko, O.G. Viagin, V.K. Klochkov, and Y.V. Malyukin, *Ukr. J. Phys.* **57**(2), 193 (2012).

26. N.V. Kononets, V.V. Seminko, P.O. Maksimchuk, A.V. Aslanov, I.I. Bespalova, A.A. Masalov, and Y.V. Malyukin, *Fiz. Nizk. Temp.* **43**, 1252 (2017) [*Low Temp. Phys.* **43**, 1009 (2017)].

27. V.K. Klochkov, N.S. Kavok, Y.V. Malyukin, A.A. Masalov, and O.G. Vyagin, *Funct. Mater.* **16**(4), 466 (2009).

28. H.Y.-P. Hong, *Acta Cryst. B* **30**, 468 (1974).

29. M. Buijs and G. Blasse, *J. Lumin.* **39**(6), 323 (1988).

30. D.F. Mullica, A.D. Grossie, and L.A. Boatner, *Inorg. Chim. Acta* **109**(2), 105 (1985).

31. B. Henderson and G.F. Imbusch, *Optical Spectroscopy of Inorganic Solids*, Oxford University Press, London (2006), Vol. 44.

32. H. Lamb, *Proceedings of the London Mathematical Society* **1**(1), 189 (1881).

33. A. Tamura, K. Higeta, and T. Ichinokawa, *J. Phys. Chem. C: Solid State Phys.* **15**(24), 4975 (1982).

––––––––––––––––––––––––